OPTIMIZATION OF THE MINOR ACTINIDES TRANSMUTATION IN ADS: THE EUROPEAN FACILITY FOR INDUSTRIAL TRANSMUTATION EFIT-PB CONCEPT

C. Artioli [1], H. Aït Abderrahim [2], G. Glinatsis [1],
L. Mansani [3], C. Petrovich [1], M. Sarotto [1], M. Schikorr [4]

[1] *ENEA, Via Martiri di Montesole 4, IT-40129 Bologna, Italy, carlo.artioli@bologna.enea.it*
[2] *SCK-CEN, Institute for Advanced Nuclear Systems, BE-2400 Mol, Belgium*
[3] *Ansaldo Nucleare S.p.A., Corso Perrone 25, IT-16161 Genova, Italy*
[4] *Forschungszentrum Karlsruhe (FZK), Postfach 3640, D-76021 Karlsruhe, Germany*

In the framework of the EUROTRANS Integrated Project the feasibility of an European Facility for Industrial Transmutation (EFIT) of Minor Actinides (MA) has to be demonstrated and the ADS reactor preliminarily designed. The core is loaded with U-free oxide fuel and cooled by lead. The actual requirements and the optimization criteria led to the so called "42-0" concept. By this approach a zero net balance of Pu is stated while the maximum MA transmutation rate of 42 kg/TWh$_{th}$ is reached, assuring a negligible BU swing of about 200 pcm/year. The about 400 MW$_{th}$ sub-critical core presents three radial zones, different either in pin diameter or in MgO inert matrix percentage, in order to maximize the average density transmutation (≈ 530 W cm^{-3} on HM) and to respect the cladding temperature limit of 550 °C. The required proton current never exceeds 20 mA at 800 MeV ($k_{eff} \leq 0.97$). Neutronic calculations have been carried out in ENEA using the deterministic code ERANOS and the Monte Carlo code MCNPX. The thermohydraulic analysis performed at FZK confirms the very promising results, making the design worth to be developed till a complete characterization.

I. INTRODUCTION

In the frame of the project IP EUROTRANS (Ref. 1) of the 6th Framework Program (FP) of the European Union, 51 European organizations have the strategic R&D objective to pursue an European Transmutation Demonstration. The aim of the 4-year lasting program is:

- To carry out the detailed design of the small size XT-ADS (eXperimental Transmutation in an Accelerator Driven System[2]), as an irradiation facility to be constructed in the short-term. The XT-ADS is also intended to be as much as possible a test facility (in lead-bismuth) for the main components and for operation of EFIT.
- To develop the conceptual design of an European Facility for Industrial Transmutation (EFIT) with a pure-lead cooled reactor of several hundreds MW with considerable Minor Actinides (MA) burning capability and electricity generation at reasonable cost. The design will be worked out to a level of detail which allows a cost study estimate.

EFIT is being designed as a transmutation demonstrator, loaded with fuel at high MA fraction. The proton beam has an energy of 800 MeV and impinges on a windowless lead target, providing the neutron source for the sub-critical system. It is intended to become operational many years after the XT-ADS (around 2040) and therefore it will take profit of the experience gained from the running European Research and Development programs on fuel and materials and of the operation of the XT-ADS.

This paper will deal mainly with the neutronic and thermohydraulic design of the EFIT core; for further details see the other EFIT article of this AccApp conference [3].

II. CORE DESIGN APPROACH

II.A. Preliminary Considerations

Burning MA is an "easy" task, in fact any nuclear system is able to fission and transmute them. In order to design the EFIT core according to its mission, it becomes crucial to well understand what is the real meaning of the mission "burning MA" (Ref. 4). In fact under the neutronic flux a part of MA is fissioned and other MA are transmuted into different isotopes (Pu). In this way new MA are created from the activated fuel, with a net balances that can range from a very few to many dozens of kg/TWh$_{th}$ of MA disappeared. Nevertheless, since the fission energy is about 200 MeV/fission, the actual overall fissioned balance must be ~42 kg/TWh$_{th}$ in any case. Of course this is the algebraic sum of the MA and Pu net balances. When the MA net balance is lower than

this value, it means that other fuel (Pu) has been fissioned too. While, when it is higher than this value, it means that a part of MA has been transmuted in new Pu instead of being burnt. In the first case the reactor acts as a Pu burner, in the second one as a Pu breeder (see the right side axis of fig. 1, where the point -50/8 is marked as an example[5]).

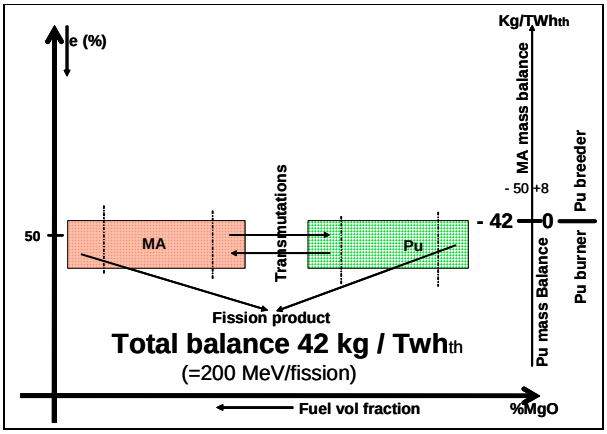

Fig. 1. MA and Pu balances.

II.B. The 42-0 Approach

The question to be answered in advance is "what about the Pu balance?".

The EFIT reactor has a U-free fuel[1], in order to avoid any production of new Pu. On the other hand, fissioning Pu in a sub-critical system, where each fission (the energy produced) is more expensive than in any MOX fueled critical reactor, implies an increase of cost per unit of MA fissioned. The conclusion is that in such sub-critical reactors each fission has to be strictly devoted, either directly or indirectly, exclusively to the MA. In term of balance it means that the MA balance has to be ~-42 kg/TWh$_{th}$, while the Pu balance will correspond to ~0 kg/TWh$_{th}$. This is called the "42-0" approach.

II.C. The Fuel Enrichment

The MA balance (and complementarily the Pu balance) depends on the ratio between MA and Pu, therefore on the enrichment (Pu/(Pu+MA)), no matter the core power, dimensions and other parameters.

The first step in designing the core has been the definition of the unique enrichment that fits the 42-0 approach. Keeping constant this figure, a suitable optimization of the core can be pursued arranging the volumetric fractions and the geometry in order to reach the desired k_{eff} (0.97) (Ref. 3) and to flat the radial distribution, both for economy and for respecting the technological constraints (mainly T_{clad} max 550°C, T_{fuel} max 1380°C).

It is important to note that, being the Pu content rather constant in the cycle, the reactivity swing will not be large. This allows to keep a rather constant proton current, avoiding an oversizing of both the accelerator and the target module.

II.D. The Optimization Approach

Optimization means of course the minimum cost per unit of MA fissioned, coupled with the minimum cost of the produced energy.

The best performance for a MA burner is 42 kg/TWh$_{th}$, no matter the reactor. In other words, it can be seen as 42 kg/h / TW$_{th}$, *i.e.* the velocity of MA fissioning per unit of power deployed is a constant. This means that the optimization must be done minimizing the cost of the TWh$_{th}$ produced, both for the side "MA burning" and for the side "energy produced". At present, waiting for economic analysis, a pseudo-optimization has led to a size of about 400 MW$_{th}$.

II.E. The Radial Flattening Technique

In the operating conditions, the mean outlet temperature of the coolant (pure lead) of 480 °C is rather close to the maximum allowed temperature of the cladding of 550 °C (Ref. 6). Therefore, the spread of the outlet temperatures of the subassemblies, belonging to the same zone of flow rate, must have a low peak factor (lower than 1.2 in first approximation). To meet this requirement the core is radially subdivided in three zones of flow rates, ruled by suitable orificing.

In order to flat the radial flux profile, the active fuel volume fraction is increased along the radius. Actually there would not be any real reason to overlap exactly the three flow rate zones over the three fuel fraction zones, but the conceptual simplicity.

Since the 42-0 approach defines univocally the enrichment, the variation of the fuel content must keep the enrichment. Two ways are possible: changing the fuel/matrix ratio, keeping the same pin and lattice, or/and changing the pin diameter in the same lattice, keeping the fuel/matrix ratio. It is evident how in this latter way, increasing the pellet volume fraction, the volume fraction of the coolant would be reduced with a loss of flow rate.

For this reason:

- the first changing, from the inner zone to the intermediate one (to equalize the fluxes), has been made by increasing the content of the reactive fuel replacing matrix material, keeping the same pin diameter (and the thermohydraulic conditions);
- the second changing, from the intermediate zone to the outer one (where the flux and the power density become quite lower anyway and less cooling is required) is made by increasing the pin diameter, keeping the same fuel composition.

II.F. The Equilibrium Core

The actual "perfect MA burner" is the reactor where only new MA are used for refueling and only fission products are unloaded. Preliminary analyses show that this as a possible scenario with EFIT. Of course for that an equilibrium composition has to be reached, in which the equilibrium vector of the plutonium is quite different from the beginning one (*i.e.* richer in even isotopes and poorer in odd ones). Nevertheless, an equilibrium enrichment exists (about 60-70%) and, more important thing, such a mixture ought to have enough reactivity to sustain an EFIT core.

III. THE EFIT CORE

III.A. Calculation Tools

The core has been designed mainly by means of the deterministic code ERANOS, with both a 2D cylindrical and a 3D hexagonal schematization. This code is able to perform fast reactor calculations including criticality, burnup and power distributions. Then, the Monte Carlo code MCNPX (Ref. 7) has also been used for two main reasons:

1. It transports both neutrons and protons at high energy (while ERANOS does not transport neither protons, nor neutrons with energy higher than 20 MeV).
2. It can calculate a detailed power distribution with a heterogeneous description of the fuel assemblies (while ERANOS uses homogenous fuel assembly descriptions). The detailed MCNPX power deposition results have then been used for the thermo-hydraulic analyses of section IV.

The methodology followed [8] was thus to use MCNPX to calculate, starting from the 800 MeV proton beam, the neutron source for ERANOS. The neutron source is defined as the first neutrons appearing in the system with energy below 20 MeV. The spatial and energy distributions of these neutrons are used as input for ERANOS.

The neutron libraries used for the codes are: ERALIB1 (Jef2.2) for ERANOS (Ref. 9) and a combination of Jeff 3.1 (Ref. 10), ENDF/B-VI (Ref. 11), LA150 (Ref. 12) for MCNPX. For high energy interactions, the CEM03 physics model[13] has been used.

III.B. Core Layout

The chosen structural material is Ferritic-martensitic steel T91, for which a maximum temperature allowed for the clad, taken into account the alluminization, is 550 °C. At present a residence time of three years is considered for the fuel. To limit the corrosion effect and meantime to have a low pressure drop through the core, the coolant speed is not higher than 1 m/s.

The fuel is a U-free one, with MgO as inert matrix. To assure the thermal conductivity in the pellet, a minimum matrix content of 50% must be used. For such a fuel a limit temperature of 1380 °C has been stated.

The isotopic compositions of the used Pu and MA are reported in table I. These vectors have been obtained as a result of a mixing of MA coming from the spent UO_2 fuel (90%) and the spent MOX (10%) of a typical PWR unloaded at the burnup of 45 MWd/kgHM, then cooled down and kept in storage for a period of 30 years. Plutonium is extracted from the same spent UO_2 but with the storage period of 15 years. With these vectors the enrichment fitting the target "42-0" has been evaluated and found to be 45.7%.

To respect the maximum fuel temperature allowed, a limiting linear power rating has been evaluated. Since the pellet thermal conductivity depends on the inert matrix content, a linear power rating of 180 W/cm has been evaluated for the pellet with 50% of matrix (minimum content, for the intermediate and outer zones) and a rating of 200 W/cm for the pellet with about 60% of matrix (for the inner zone).

The dimension and the composition of the pin and of the fuel assembly are shown in figs. 2, 3 and 4. While the pin diameter and the pitch derive from thermal balance, the fuel assembly dimensions are driven by the size of the spallation module, that has to be inserted replacing the 19 central assemblies[3]. Gathering different kinds of fuel element (inner, interm., outer) for reaching the required reactivity and adjusting the diameters and the matrix content, the core shown in fig. 5 has been laid down.

TABLE I. MA and Pu weight compositions

MA	[w%]	Pu	[w%]
^{237}Np	3.884	^{238}Pu	3.737
^{241}Am	75.510	^{239}Pu	46.446
^{242m}Am	0.254	^{240}Pu	34.121
^{243}Am	16.054	^{241}Pu	3.845
^{243}Cm	0.066	^{242}Pu	11.850
^{244}Cm	3.001	^{244}Pu	0.001
^{245}Cm	1.139		
^{246}Cm	0.089		
^{247}Cm	0.002		

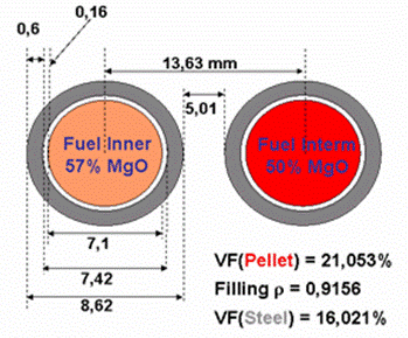

Fig. 2. Pins for the inner and intermediate zones.

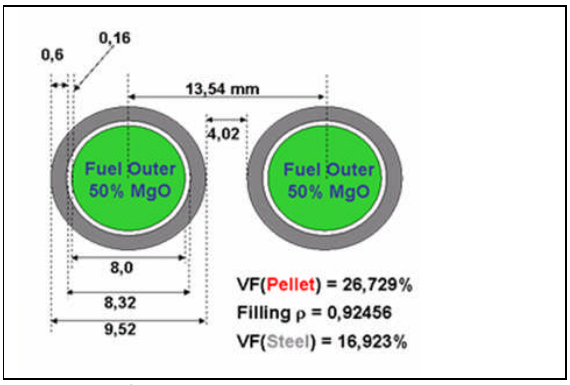

Fig. 3. Pin for outer zones.

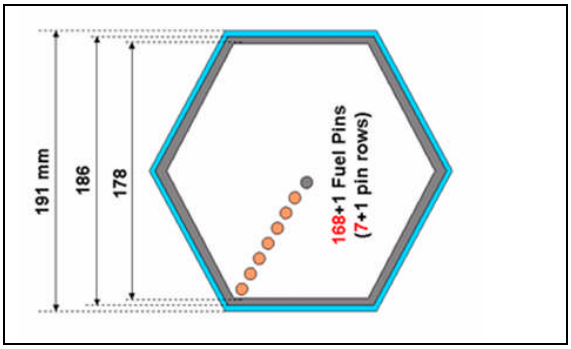

Fig. 4. Hexcan for all zones.

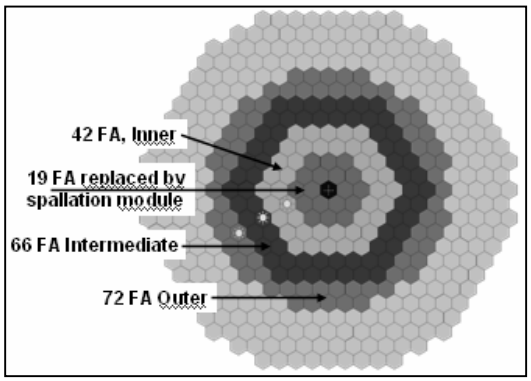

Fig. 5. The 3-zones EFIT core (180 fuel assemblies).

III.C. Power Distribution

The flux radial flattening aims to reduce as much as possible the radial form factor within each radial zone, and to reach the maximum power density peak allowed.

Figure 6 shows the power density radial profile, on the peak plane (about midplane), obtained in RZ geometry.

Related to the two different allowed linear power ratings (200 W/cm and 180 W/cm) the corresponding limits on the homogeneized power density have been calculated and marked on the figure (106 W/cm^3 for the Inner zone and 97 W/cm^3 for the Intermediate and Outer zones). The slight exceeding of the peak in the Intermediate zone will be surely eliminated when, by 3D calculations, a more precise zone contour will be defined.

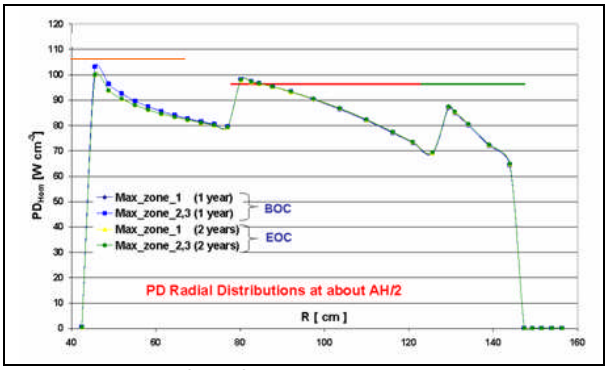

Fig. 6. Radial profile of the homogeneous power density.

In the third zone the peak does not reach the maximum. The geometrical peripheral decreasing of the flux is not fully compensated by the pin diameter increasing, notwithstanding this synergically both sustains the flux and increases the fissile mass per length of the pin. Increasing more the diameter could improve the power density but it will drag an unacceptable reduction of the coolant flow and an increase of the outlet T (as discussed in the previous II-E).

The overall power (beam excluded) of the core is 389 MW_{th}, 5 MW_{th} of which are dissipated in structural zones outside the active core. The average homogeneous density power is 70.7 W/cm^3.

Table II collects, for the Beginning Of Cycle (BOC) and End Of Cycle (EOC), the power in the hot and mean FA in the 3 zones: Inner, Intermediate and Outer (index 1,2,3). The form factors, both radial and axial in the three zones, are shown in Table III.

TABLE II. Hot and mean FA power in the 3 zones

MW_{th}	P_{thmax1}/FA	P_{thmax2}/FA	P_{thmax3}/FA	$AveP_{th1}$/FA	$AveP_{th2}$/FA	$AveP_{th3}$/FA
BOC	2.57	2.43	2.43	2.29	2.16	1.95
EOC	2.58	2.48	2.47	2.26	2.16	1.96

TABLE III. Radial and axial form factors in the 3 zones

	ff_{rad} inner	ff_{rad} intermediate	ff_{rad} outer	ff_{ax} inner	ff_{ax} intermediate	ff_{ax} outer
BOC	1.12	1.13	1.24	1.14	1.16	1.17
EOC	1.14	1.15	1.26	1.14	1.16	1.17

As clearly shown in fig. 6, while the radial form factors (actually the ratio between the hot assembly to the mean one) are quite satisfactory in the Inner and Intermediate zones, in the Outer zone they appear too high. This is essentially due to the fact that, in cylindrical schematization, the contour of the zones follows a “radius law” rather than the actual released power. As exposed

below, a more precise contour of the zone could reduce the radial factor within the desired limit.

III.D. Reactivity Swing

The residence time is stated in three years, life time that allows to reach the peak burn up of about 10% (Ref. 1), within the limit imposed by the corrosion and well below the dpa limit. This span of time is divided into three subcycles 1 year long.

Due to the rather constant content in Pu during the irradiation the reactivity swing is very small, 200 pcm/year (fig. 7), *i.e.* some 6% of the subcriticality (3000 pcm), that accounts for a little spread of the proton current required.

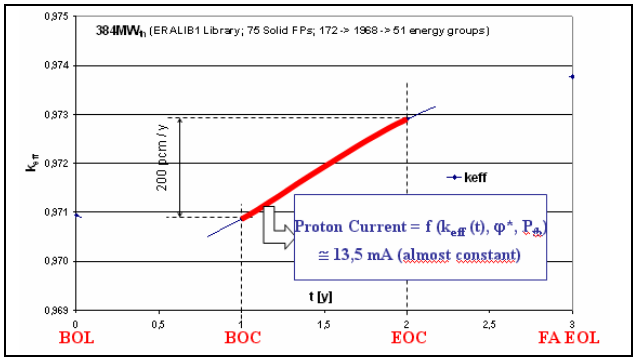

Fig. 7. Cycle reactivity swing.

III.E. Burning Performances

Figure 8 shows the mass evolution of the MA and Pu during the irradiation. As consequence of the selected enrichment, 45.7% (42-0 approach), the mass of the Pu remains rather constant, while only the MA are fissioned. Of course this does not mean they are all "directly" fissioned, nevertheless the overall effect is the same.

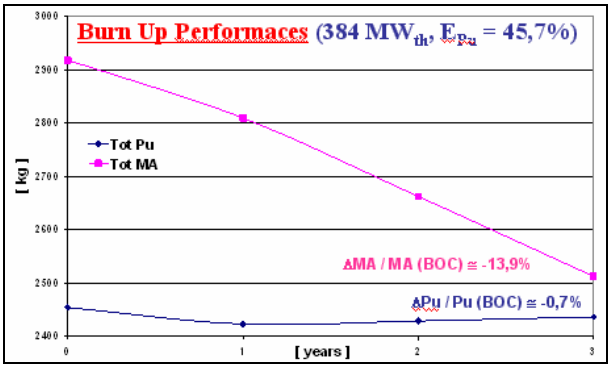

Fig. 8. MA and Pu evolution during the fuel life.

Table IV shows the burning performance during three years of staying in the core.

TABLE IV. Burning performance

3 years	BU = 78,28 MWd / kg (HM)	BU	-40,17 kg (MA) / TWh
	Total E = 10,0915 TWh$_{th}$		-1,74 kg (Pu) / TWh

III.F. MCNPX Results

The whole system, including the target and the core, has been modelled for MCNP in a very detailed 3D geometry (including thermal expansions and neutron libraries at different temperatures). The analysis has been performed at BOC and the main integral parameters are reported in table V.

TABLE V. MCNPX results at BOC
(the error is the standard deviation)

k_{eff}	0.97403 ± 0.00023
Neutron source (S) (neutrons/proton)	23.02 ± 0.08
M= all fission neutrons / S	19.45 ± 0.25
$k_S = M / (M+1)$	0.95111 ± 0.00059
$\varphi^* = \frac{(1-k_{eff})/k_{eff}}{(1-k_S)/k_S}$	0.52
Proton current	13.2 mA

There is a discrepancy of ~930 pcm in k_{eff} between ERANOS (with the ERALIB1 library) and MCNPX (with the Jeff 3.1 library). The MCNPX results using the ENDF/B-VI library appear to be more similar to ERANOS (320 pcm of difference in k_{eff}). Note that the neutron source efficiency is φ*=0.52, while in the PDS-XADS design was φ*=0.99 (k_S and k_{eff} very similar)[14]. This effect is mainly due to the different fuel composition and to the larger radius of the target.

The power deposition distribution in each assembly of the core, separated per ring, is shown in fig. 9 (the periodic behaviour reflects the symmetry in the hexagonal geometry).

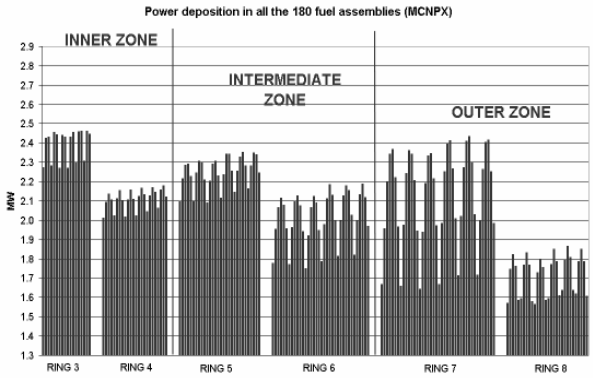

Fig. 9. Power deposition distribution in each assembly (the standard deviation of the Monte Carlo calculation is <2.5%).

From these results, the 3 hottest assemblies in the 3 zones have been identified, together with the axial form factors and the value of the heat release in the hottest pin (16.4 kW). The maximum linear power in the fuel pins turns out to be 203 W/cm. The axial profiles have been calculated for the 3 average and 3 hottest assemblies. The differences with ERANOS are within 5% for the hottest assemblies and within 3% for the axial form factors. As a result of this analysis, better zone contours can be defined, mainly for the Intermediate/Outer interface. In fact, replacing the FA in the Outer zone in the "peak places", with Intermediate FA (and viceversa *mutata mutandis*), significant radial factors and mean density power improvements are obtained.

All the MCNPX results are used for the thermal-hydraulic analyses.

IV. THERMAL-HYDRAULIC ANALYSIS

The preliminary results of the thermal-hydraulic analysis of the core are reported in this section. These analyses were performed with the static version of the SIM-ADS code for each of the three core zones.

Calculated for each core zone are the expected axial and radial temperature distributions within the fuel pin and the sub-assembly for the average and the peak power fuel pins for axial power distributions calculated by MCNPX. Two core conditions are analyzed, namely Beginning-Of-Cycle (BOC) and End-Of-Cycle (EOC).

The thermal conductivity of the two different MA-fuel compositions, namely MgO volume fractions of (CZ1/CZ2/CZ3 = 57%,50%,50%), were calculated based on the known thermal conductivities of MgO and MOX-MA-fuels using the Bruggeman weighting scheme and applying an appropriate correction for burnup. More details of this procedure can be found in (Ref. 15).

Under BOC conditions, fresh fuel conditions are presumed. Under nominal conditions, the size of the gap between clad and fuel has closed down to about 110 μm for the average pin, or about 70% of the cold condition value, and the gas composition in the gap is dominated by He, namely (He/Xe/Kr = 0.976/0.023/0.001).

Under EOC conditions, a peak fuel burn-up of about 100 MWd/kg has been assumed for these calculations. The gap between clad and fuel is presumed to be essentially closed (min gap ~ 4 μm) and the fission gas composition in the gap is still dominated by He due to the higher helium fission gas production in MA fuel compared to conventional fuel (factor ~3.6 has been calculated), namely (He/Xe/Kr = 0.781/0.201/0.017). For the peak pins, pin pressures of (CZ1/CZ2/CZ3= 112/116/127) bars are calculated.

An additional parameter requiring closer attention in the thermal hydraulic analysis is the formation of an oxide layer on the cladding material. The formation of this oxide layer serves a protective function against clad corrosion, on the one side; on the other side it will impede heat transfer from the clad surface to the coolant. A maximum layer thickness of 5-10% of the cladding thickness can be presumed as a guiding parameter for EOL analysis. Several oxide layer thicknesses, namely 100, 200, and 300 μm, have been used as a parameter in our analysis. The thermal conductivity of the oxide layer is assumed to be ~ 1 W/m/K.

To assure a uniform pressure drop across the entire core, orificing of core zones 1 and 2 are required. Assuming 6 axial grid spacers of thickness 0.20 mm, unorificed core pressure drops of (CZ1/CZ2/CZ3 = 0.178/0.162/0.233) bar are calculated.

The analyses were performed for two plant conditions, namely nominal operations (100% load) and steady state ULOF conditions. A height differential between core and heat exchanger of 3.70 m has been assumed for these calculations as well as a system pressure loss factor Z = 1.38 (ratio of system pressure drop to core pressure drop).

Tables VI and VII summarize the results of these calculations. Under nominal BOC conditions, peak fuel and peak clad temperatures are well within acceptable upper limits for all 3 core zones, namely ~ 1380 °C for the fuel and about 550 °C for the cladding.

Under EOC conditions the acceptability depends on the actual thickness of the oxide layer.

TABLE VI. Summary of the thermal-hydraulic Analysis

			EFIT - Pb : Peak Fuel and Cladding Temperatures [°C]											
			Inner Core Zone CZ1				Intermediate Core Zone CZ2				Outer Core Zone CZ3			
		Oxide Layer thickness	Avg Pin		Peak Pin		Avg Pin		Peak Pin		Avg Pin		Peak Pin	
			Clad	Fuel	Clad	Fuel	Clad	Fuel	Clad	Fuel	Clad	Fuel	Clad	Fuel
Nominal Conditions	BOC	0 μm	505	1220	530	1399	503	1242	519	1365	497	1133	531	1394
	EOC	0 μm	505	824	539	1006	503	842	523	953	497	786	526	933
		100 μm			600	1126			580	1058			571	1025
		200 μm			677	1241			650	1160			631	1117
		300 μm			758	1347			722	1258			695	1206
ULOF Conditions	BOC	0 μm			675	1475			652	1436			692	1473
	EOC	0 μm			689	1149			660	1086			685	1083
	EOC	100 μm			743	1259			705	1185			726	1170
	EOC	200 μm			797	1361			758	1279			767	1255
	EOC	300 μm			868	1457			832	1367			816	1336

Under ULOF and BOC conditions, both peak cladding and peak fuel temperatures will remain under the respective temperature limits.

Under ULOF and EOC conditions, an upper limit of 100 μm oxide thickness (15% of the clad) seems to be required in order to prevent peak clad temperatures to exceed the 710 °C limit. In case the layer thickness should approach 200 – 300 μm, clad failure time of less 0.5 hours are observed (see Table VII).

Based on the above results, the current Pb-cooled EFIT design seems quite viable. Attention needs to be placed however on the operational control of the oxygen content in the Pb coolant in order to control chemical fowling and the buildup of the oxide layer.

TABLE VII. Calculated Clad Failure Times under Nominal and ULOF plant conditions

			EFIT - Pb : Cladding Failure Times [hrs]					
		Oxide Layer thickness	Inner Core Zone CZ1		Intermediate Core Zone CZ2		Outer Core Zone CZ3	
			Avg Pin	Peak Pin	Avg Pin	Peak Pin	Avg Pin	Peak Pin
Nominal Conditions	BOC	0 μm	E11	E10	E11	7.0XE10	E11	E10
	EOC	0 μm	E9	E6	6.8XE8	2.5xE7	6.9xE8	5.2xE6
	EOC	100 μm		7.0XE4		1.90E+05		1.1xE5
	EOC	200 μm		4.5xE4		1.0xE3		1.2xE3
	EOC	300 μm		1.44		9.8		17.4
ULOF Conditions	BOC			2XE10		5.5xE5		3.0xE4
	EOC	0 μm		66.7		371		23.9
	EOC	100 μm		2.57		208		2.02
	EOC	200 μm		0.14		0.97		0.21
	EOC	300 μm		0.3 min		2.0 min		1.0 min

V. REACTIVITY FEEDBACK COEFFICIENTS

The core is characterized by the missing of the Doppler prompt reactivity feedback, due to the lack of ^{238}U in the fuel. Moreover this core is also characterized by a very low delayed neutrons effective fraction, due to the large content in MA. MCNPX results show that:

- at BoC: $\beta_{eff} = 0.00148 \pm 0.00037$;
- at EoC: $\beta_{eff} = 0.00163 \pm 0.00037$.

Concerning the reactivity variation for unitary relative variation of the atomic density of a given material, the results are:

– for the whole active core flowing coolant, a "reactivity worth" of - 0.058,

– for the whole active core cladding, a "reactivity worth" of - 0.038,

– for the whole active core, the fuel (Pu) reactivity worth it is about 0.47.

For the coolant void effects, the following results were obtained:

Whole Active Core:

– ***BoL:*** $(\Delta k/k)_{eff} = + 0.06884 \pm 0.00041$,

– ***BoC:*** . $(\Delta k/k)_{eff} = + 0.06666 \pm 0.00039$,

– ***EoC:*** . $(\Delta k/k)_{eff} = + 0.06387 \pm 0.00040$;

Whole Active Core + Upper Plenum:

– ***BoC:*** . $(\Delta k/k)_{eff} = + 0.05609 \pm 0.00039$,

– ***EoC:*** . $(\Delta k/k)_{eff} = + 0.05297 \pm 0.00041$,

Whole Active Core + Upper and Lower Plena:

– ***BoC:*** . $(\Delta k/k)_{eff} = + 0.03773 \pm 0.00041$,

– ***EoC:*** . $(\Delta k/k)_{eff} = + 0.03464 \pm 0.00040$.

The above results show the huge penalisation arising from the "hyper-conservative" hypothesis of the core voided, keeping the coolant in the plena.

Figure 10 shows the ring by ring void effect distribution and the radial distribution by FA. It is clear as the void effect is everywhere positive, except in the last outer ring where is nearly zero.

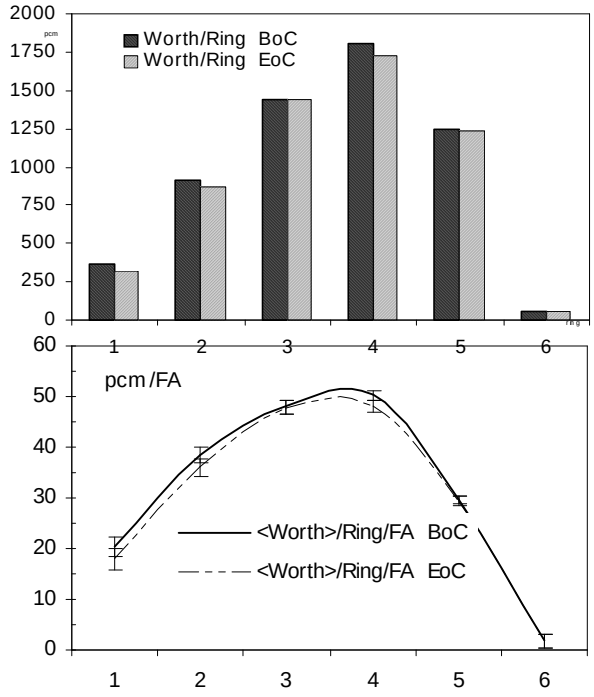

Fig. 10. Void effect.

VI. HEAT RELEASE IN THE TARGET

The power of a 800 MeV proton beam is 800 kW/mA, but this does not correspond to the power deposition in the Pb target: part of it can be carried out by the kinetic energy of the secondary particles and part can be lost in changing the mass of the target nuclei.

MCNPX calculations show that, with 1 mA of proton current, 581 kW are deposited in the target circuit, corresponding to 73% of the beam power. In this configuration about 6% of the beam power is carried out by the secondary particles (mainly neutrons) that escape the target.

A MCNPX simulation has also been performed to reproduce the experimental value reported in (Ref. 16), where a 800 MeV proton impinges on a lead cylinder of 10 cm radius. The agreement between the results is found to be within 8%, that is lower than the quoted experimental error of 10%.

If, during the life of the system k_{eff} is always >0.97, then the proton current is estimated to be at maximum 15.4 mA and the heat deposition in the target at maximum 9 MW. Since the target has been designed to withstand to higher powers, if it is dimensioned to this new value (9 MW), the radius of the spallation module might be decreased in order to improve the efficiency of the neutron source. As a matter of fact, the target moderates the spallation neutrons while higher energy neutrons would be more efficient in feeding the sub-critical core.

VII. CONCLUSIONS

The transmutation (fission) of MA, via a U-free lead cooled ADS, has been demonstrated to be promising by the EFIT concept. The "42-0" approach, where each fission is strictly devoted (either directly or indirectly) to the MA, has been stated. It has been demonstrated how the optimizations of the MA burning and energy production, instead of being in conflict, are driven by the same parameter, that is the cost of the energy production. Even if the safety analysis has not been carried out yet, the core fundamental parameters and the plant design[3] indicate that the safety requirements are fulfilled. Nevertheless R&D effort is required, mainly for the qualification of the steel cladding in lead environment (at the exercise temperature) and of the U-free fuel with high content of MA.

ACKNOWLEDGMENTS

The authors thank the Partners of the IP-EUROTRANS project for their fruitful contribution to the project. Special thanks to the European Commission for the financial support through the FP5 and FP6 programs.

REFERENCES

1. J. KNEBEL et al., "EUROTRANS: European Research Programme for the Transmutation of High-level Nuclear Waste in an Accelerator-driven System," *Ninth Information Exchange Meeting*, Nimes, France, September 25-29, 2006.
2. D. DE BRUYN, B. GIRAUD, D. MAES, L. MANSANI, "From MYRRHA to XT-ADS: the design evolution of an experimental ADS system," *ACCAPP'07*, Pocatello, Idaho, USA, 30 July – 2 August, 2007.
3. A. BARBENSI, C. CORSINI, L. MANSANI, C. ARTIOLI, G.GLINATSIS, "EFIT: the European Facility for Industrial Transmutation of Minor Actinides," *ACCAPP'07*, Pocatello, Idaho, USA, 30 July – 2 August, 2007.
4. C. ARTIOLI, "Specification for the EFIT Core and Fuel Element," FP6, IP EUROTRANS, D1.6, 2006.
5. C. ARTIOLI, "A-BAQUS: a multi-entry graph assisting the neutronic design of an ADS," *5th International Workshop on the Utilization and Reliability of High Power proton Accelerator*, Mol, Belgium, May 6-9, 2007.
6. "A Technology Roadmap for Generation IV Nuclear Energy Systems", GIF-002-00, USDOE Nuclear Energy Research Advisory Committee and the Generation IV International Forum (2002).
7. J.S. HENDRICKS et al., *MCNPX, Version 26C*, Los Alamos National Laboratory report LA-UR-06-7991, December 2006.
8. K.W. BURN, *A Decoupled Approach to the Neutronics of Sub-Critical Configurations: Evaluating the Neutron Source*, RT/ERG/99/2, ENEA, Bologna, Italy (1999).
9. G. RIMPAULT et al., "Schema de Calcul de Reference du Formulaire Eranos et Orientations pour le Schema de Calcul de Projet", CEA XT-SBD-0001, August 1997.
10. The Jeff-3.1 Nuclear Data Library, Jeff Report 21, NEA (OECD 2006), ISBN 92-64-02314-3.
11. R. ORSI, M. PESCARINI, A.I. BLOKHIN, *MCB6.BOLIB – An ENDF/B-VI Release 3 Cross Section library for the MCNP Monte Carlo Code*, KT-SCG-0004 Rev. 0, ENEA, Bologna, Italy (1999).
12. M.B. CHADWICK et al., *Nuclear Science and Engineering* **131**, *3*, 293 (1999).
13. S.G. MASHNIK et al., "CEM03.S1, CEM03.G1, LAQGSM03.S1, and LAQGSM03.G1 Versions of CEM03.01 and LAQGSM03.01 Event-Generators," Los Alamos National Laboratory report LA-UR-06-1764 (2006), http://mcnpx.lanl.gov.
14. K.W. BURN, G. GLINATSIS, L. MANSANI, E. NAVA, C. PETROVICH, M. SAROTTO, "Preliminary Nuclear Design Calculations for the PDS-xADS LBE-Cooled Core," *Proceedings of the International Workshop on P&T and ADS Development*, Mol, Belgium, October 6-8, 2003.
15. W. MASCHEK et al., "A Comparative Assessment of Safety Parameters and Core Behavior for the CERCER and CERMET Oxide Fuels Proposed as EFIT (intermediate Report)", WP3.2, DM3 AFTRA, Deliverable 3.1, March 2007.
16. V.I. BELYAKOV-BODIN et al., *Nuclear Instruments and Methods in Physics Research* A295, 140 (1990).